Journal of Applied Science and Engineering, Vol. 21, No. 2, pp. 179–186 (2018) DOI: 10.6180/jase.201806_21(2).0005

Low-cost Test Rig for Aerodynamic Evaluation of Ornithopters

Balasubramanian E[1]*, Sasitharan A[2], Chandrasekhar U[1], Karthik K[3] and Lung-Jieh Yang[4]

[1]Vel Tech University, Avadi, Chennai
[2]Bubblefly Technology Pvt Ltd, New Delhi
[3]Madras Institute of Technology, Chennai
[4]Department of Mechanical and Electromechanical Engineering, Tamkang University, Tamsui, Taiwan 251, R.O.C.

Abstract

Experimental assessment of lift and thrust forces of flapping wing micro aerial vehicles (FWMAVs) is of paramount interest to assess its payload carrying capability. In this work, a simple and cost effective test bench is developed to measure the forces of ornithopter. Two compressive load cells are calibrated and assembled in an appropriate mode to capture the generated forces. A labview based graphical user interface is designed to acquire real time force data and thereby control the angle of attack of ornithopter. Through varying wind speeds, flapping frequencies and angle of attacks (AOA), wind tunnel experiments are conducted for two ornithopters E-Bird and Golden Snitch, with wing spans of 27 cm and 21.5 cm respectively. Experimental results suggested that, E-Bird has attained maximum lift force of 28.7 g at 60° AOA and golden snitch has 13.5 g lift force at 35° AOA. The developed compact test rig can measure the lift and thrust forces upto 200 grams with an accuracy 0.1 gram of FWMAVs.

Key Words: Ornithopter, Lift and Thrust Forces, Load Cells, Data Acquisition, Wind Tunnel, Graphical User Interface

1. Introduction

FWMAVs or ornithopters, are becoming popular for surveillance and reconnaissance applications [1]. The inherent characteristics such as efficient gliding, perching, hovering and maneuvering in confined spaces attracted many researchers. FWMAVs are capable of changing aerodynamic needs through their flight characteristics. They can vary the angle of attack, wingtip trace pattern, wing area, flapping frequency and adjusts feather orientation to achieve cruising and forward flights. It has the capability of carrying out several missions in indoor as well as outdoor locations. A comprehensive review on directional control of flapping wing vehicle, flapping mechanisms and various wing designs can be seen in [2]. The aerodynamics of ornithopter is non-linear, complex, and a quite difficult to model. The flapping of the wing creates an unsteady airflow around the control surface of the bird which increases the complexity of aerodynamics [3–6]. In order to obtain a smooth flight, the lift to weight ratio has to be greater and thrust of the FWMAV has to overcome the drag effects for efficient forward flight. Ornithopters are very dynamic systems which generates huge amount of vibration during its operation. Hence, it is important to have a specialized and sophisticated system to measure the flight parameters of the FWMAVs. Measurement of aerodynamic forces are of prime importance to determine the payload capacity. In the literature, few test rigs are developed to measure the performance characteristics of Ornithopters. Dae-Kwan Kim et al. [7] conceptualized a test rig. It consists of driving part, a test mount and a measurement part through which aerody-

*Corresponding author. E-mail: esak.bala@gmail.com

namics forces are measured. M. Y. Zakaria, et al. [8] constructed a strain gage measurement system supported by three struts to ensure a strong base from the ground. The aerodynamic forces are measured relative to the body-axes and mapped to wind axes in the wind tunnel setup which in turn gives the thrust as well as lift forces. R. J. Wood [9] developed a test rig to measure the micro level forces of Ornithopters. The average lift is measured from 10 trials is in the order of 1.14 ± 0.23 mN. University of Maryland [10] built a rig consists of aluminium base plate attached to the top of reinforced PVC pipe by means of aluminium slugs. A strain gauge transducer with 6 DOF is embedded between a test stand and a vice. The transducer is used to measure the vertical and horizontal forces during the flapping motion of an Ornithopter. P. Daniel Kuang et al. [11] simulated various wing motions such as pitching, flapping and lead-lag. The eight degrees of freedom (DOF) test bed has three joints in each shoulder and two joints for the amplitude of flapping. Using these DOF, lead-lag, flapping, and pitching are determined. Curtis et al. [12] used air bearing thrust strand with a 6-axis component load cell to measure thrust forces for various wing spans of one degree of freedom flapping wing mechanism. Figure of merit and maximum amount of power required for FWMAV are calculated. The axial and normal forces are measured for various flapping frequencies. Park et al. [13] designed a flapping wing force measurement system using Nano 17 six axis load cell with a resolution of 0.078 g and maximum allowable range of force 1200 g. Three sections of data acquisition idle 1, flapping time and idle 2 are considered. The lift and thrust forces are measured 20 different time intervals and average force is accounted. Recently, few researchers utilized six axis balance for measuring the lift and thrust forces of ornithopter [14–16]. It can be inferred from these literature that, most of the researchers have used 6 axis component load cells which are costly. The present work focuses on low cost aerodynamic characteristics measurement using cost effective load cells and data acquisition systems to measure the lift and thrust forces of ornithopter.

2. Design and Fabrication of Ornithopter Test Rig

Generally, the air flow field around flapping wings is unsteady. A large angle of attack would lead to flow separation and turbulences. This unsteady aerodynamics may not be explained by common airfoil theory.

The airfoil is selected based upon the specifications stated by The National Advisory Committee for Aeronautics (NACA). The NACA 0030 airfoil is symmetrical which smoothen flow (smoke test) of the wind inside the wind tunnel without disturbing the rod on which the ornithopter is mounted. The CAD model of airfoil section (Figure 1) and solid bar to connect ornithopter is shown in Figure 2.

The airfoil is fabricated using glass fiber and aluminium which are shown in Figure 3(a) and (b). Compared to aluminium cross section, glass fibre has obtained good surface finish. Two layers are made with an inside layer being glass fibre and the outer layer of carbon fiber for pleasing appearance. It is made in such a way that the surface remains smooth at all the times. The fabricated aerofoil with bottom support structure is shown in Figure 4. Initially, to achieve connectivity between fuselage and load cells various configurations are attempted. The arrangement of strings attached to the fuselage Figure 4(a) and a rod which is attached and extended below from the golden snitch ornithopter is shown in Figure 4(b).

In order to accommodate the load cells, data acquisi-

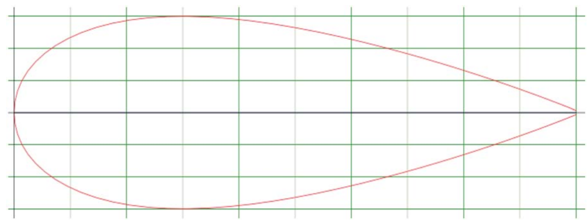

Figure 1. Constructed aerofoil sections.

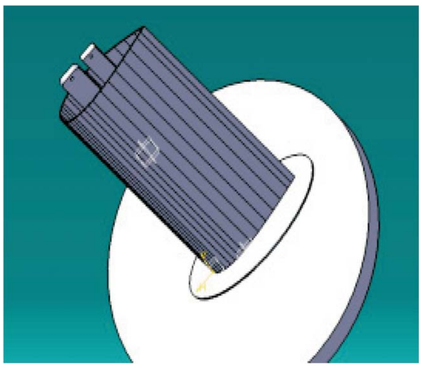

Figure 2. A solid bar and aerofoil section.

tion (DAQ) systems and provision for easy handling of electronic parts, a conceptual model shown in Figure 5(a) is proposed. Load cells, indicators, NI DAQ systems, and Arduino micro controller components are placed inside the base and each of the port is made accessible through the USB cables. Servo motor is mounted on the top aluminium square rod, which helps to attach ornithopter with the test rig system. A 10 mm thick acrylic glass sheet is used to build the bottom support structure so that the user can have visual access to the data handling system. The fabricated model of test rig is shown in Figure 5(b)

3. Load Cell Calibration and Data Acquisition

Two 200 g range Wheatstone bridge strain gauge uniaxial load cells as shown in Figure 6(a) with an accuracy of 0.1 g are used to measure the lift and thrust forces. A National Instrument (NI) Lab View data acquisition system is incorporated to acquire the data from load cells. In order to calibrate the load cells and make useable conclusions from the data, known loads are applied to the sensors as shown in Figure 6(b).

The calibrated curve shown in Figure 7 confirms that it has good linear relationship between the applied load and the generated voltage. The calibrated data constants from both the load cells will be utilized as multiplication factor to convert the real time voltage signals into the forces produced by the ornithopter.

3.1 Control of Angle of Attack

Arduino based microcontroller setup is integrated to control the angle of attack of ornithopter. The schematic

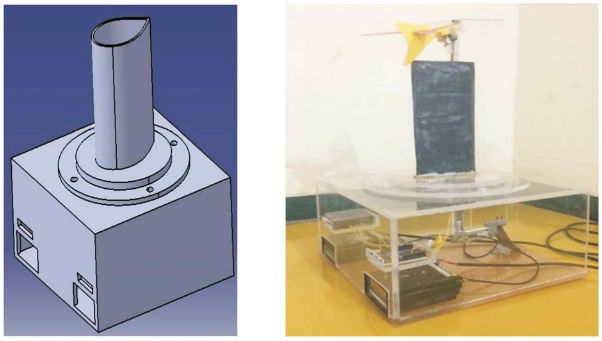

a) Conceptual model of test rig b) Fabricated rig

Figure 5. Developed test rig

a) Glass fiber b) Aluminium

Figure 3. Fabricated aerofoils.

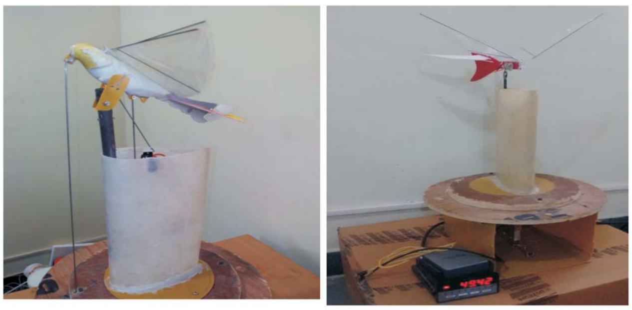

a) Strings connected b) Rod connected

Figure 4. Connectivity between fuselage and load cells

a) Arrangement of load cells b) Calibration of load cell

Figure 6. Load cells and its calibration.

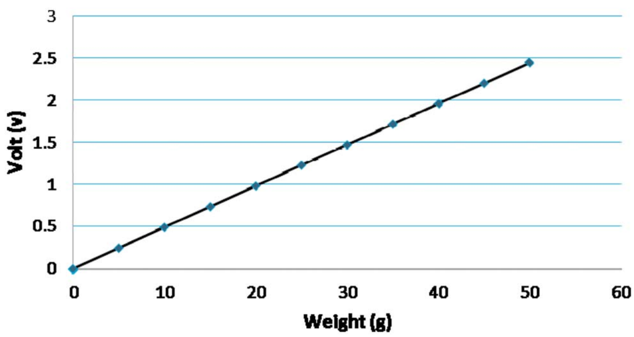

Figure 7. Calibration curve.

representation of servo actuated control of Ornithopter angle of attack (AOA) is shown in Figure 8.

In order to change the angle of attack in real time, a Lab view based control panel is designed and depicted in Figure 9. Micro controller is programmed in such a way that control signals will be sent to servo motor attached to the ornithopter through USB port. While adjusting the knob to vary the angle of attack, the corresponding program is executed in arduino micro controller, which in turn sends the pulse width modulated control signal to the servo motor. The Figure 10 shows ornithopter at various tilted positions of structure and there will be a feedback from the servo motor, which in turn provides the angle of tilt considered as AOA based on user input in the developed graphical user interface (GUI).

4. Wind Tunnel Testing and Discussions

The measurement of lift and thrust forces of FWMAV has been carried out in room conditions and in the wind tunnel facility available at Aerodynamics Laboratory, Vel Tech University, India. The facility is a sub sonic suction type with cross section of 600 × 600 mm and a length of 2000 mm as shown in Figure 11. The contraction ratio is 1:3 and the maximum air speed in the wind tunnel can be obtained is 50 m/sec. Present study considers two ornithopter configurations, a commercial model called E-Bird (27 cm wing span weighs 14 g) and a university micro aerial vehicle called Golden Snitch [17] (21.5 cm wing span weighs 10 g).

In order to neglect the wall effects, blockage ratio (BR) is calculated. It is calculated as the ratio between frontal projected area of FWMAV to the wind tunnel cross sectional area that is to be kept less than 10% [18]. Hence, for various angles of attack (AOA), blockage ratio is determined and depicted in Figure 12. It is observed that, BR is within the maximum limit and internal effects of air will not affect the force measurement.

During the wind tunnel experimentation, wind velocity is measured with the aid of an anemometer (Figure 13(a)) and environmental meter (Figure 13(b)). The volt-

Figure 8. Arduino based control of AOA.

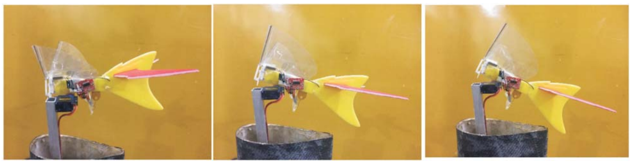

Figure 10. Golden snitch at various AOA (0°, 10°, 20°).

Figure 11. Ornithopter test rig assembled in wind tunnel test section.

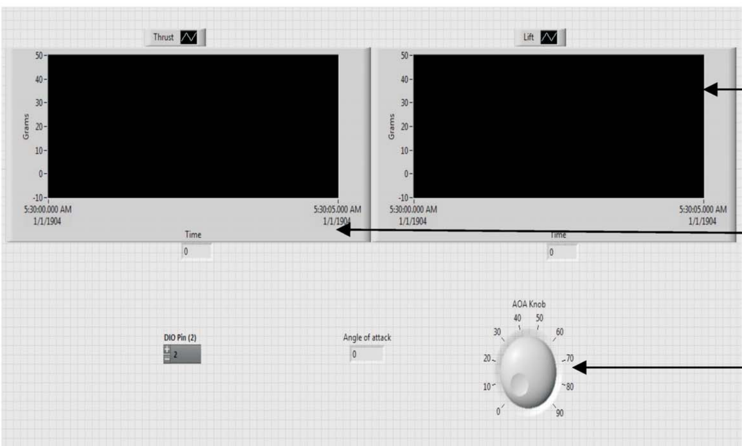

Figure 9. Graphical user interface for on-line monitoring.

age variation provides speed control of motor which in turn actuate the flapping mechanism and the voltage is measured using multimeter as shown in Figure 14(a). The flapping frequencies for various voltage signals (11.5 Hz, 13.0 Hz, 14.5 Hz, and 17.2 Hz) are measured using stroboscope as shown in Figure 14(b).

The complete lay out and procedure of lift and thrust forces measurement is depicted in Figure 15.

4.1 Force Measurement for E-Bird

An E-Bird is rigidly mounted on the test rig and measurement of lift and thrust forces have been carried out in the wind tunnel. It can be observed from Figure 15 that, the increase in wind speed and AOA leads to increase in lift force. As AOA increases from 0° to 60°, the lift force slightly increases and further increase in AOA results in decreasing of lift force because of drag. It can be observed that in the region of AOA 60°-70°, higher lift force will be generated in E-Bird. However, when AOA increases thrust decreases. It is due to the predominant effect of drag force that can be seen in Figure 16.

4.2 Force Measurement of Golden Snitch Ornithopter

Similar experimentations have been performed to

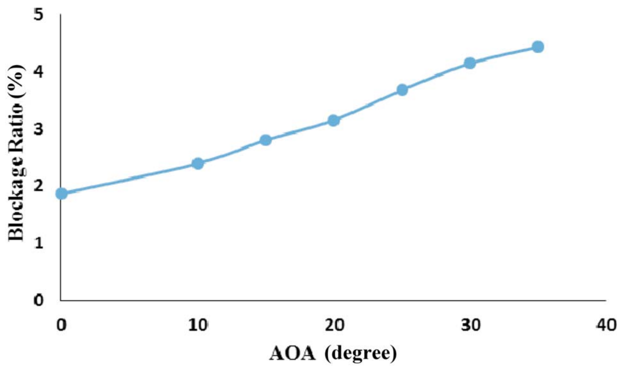

Figure 12. Blockage ratios for various AOA.

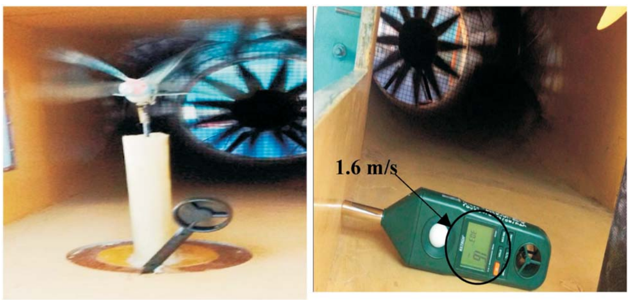

a) Anemometer b) Environmental meter

Figure 13. Measurement of wind velocity.

a) Measurement of voltage b) Stroboscope

Figure 14. Measurement of flapping frequency.

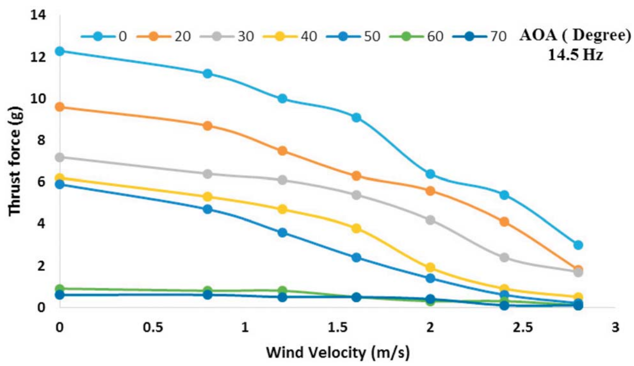

Figure 16. Effect of wind velocity and angle of attack on thrust force.

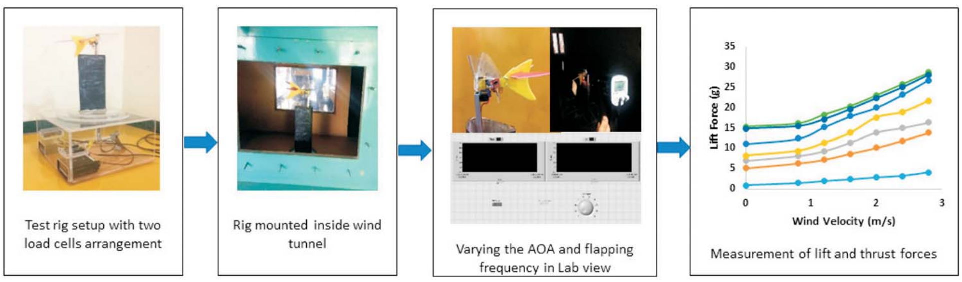

Figure 15. Lay out of ornithopter force measurement.

determine the lift and thrust forces of golden snitch ornithopter. The trend of increasing lift force with the increase of AOA can be observed in Figure 17 and similar aerodynamic characteristics can be seen in [19,20]. At wind velocity of 2.8 m/sec for the increase in AOA, golden snitch ornithopter experienced zero or negative thrust. However, lift force dominated more and maximum of 13.5 g force is generated. Similar trend can be also observed in [20] at wind velocity 2.8 m/sec. Further increase in wind speed produces negative thrust, which is not shown in Figure 18. Hence, the golden snitch ornithopter is found to be suitable for indoor applications where the wind velocity is less than 2.8 m/sec. The effect of side forces on lift and thrust is not accounted. Rolling, pitching and yawing moments are not also not measured.

4.3 Comparative Studies with Golden Snitch Ornithopter

In order to verify the results of lift and thrust forces generated from developed test rig with the upshots of [20] from Tamkang University, comparative studies are performed. At 39.6° stroke angle, S2 wing configuration and for various flapping frequencies experiments are conducted. It can be seen from Figure 19(a)–(f), similar trend is observed in lift as well as thrust forces for both the cases.

A sudden drop in thrust occurs around 1–1.5 m/s as the local turbulence induced frequency change matches with the flapping frequency of ornithopter. As the velocity increases further, the frequency shift in turbulence is slightly higher and it allows overshooting of the range and hence the thrust reduction becomes linear. The error percentage between actual and reference is maintained about 20% for lift force and higher error occurs for the thrust force at low wind velocity and it is reduced to about 20% while increase in wind velocity as observed in Figure 19. However, developed test rig yielded higher thrust force than that of the results from Tamkang University.

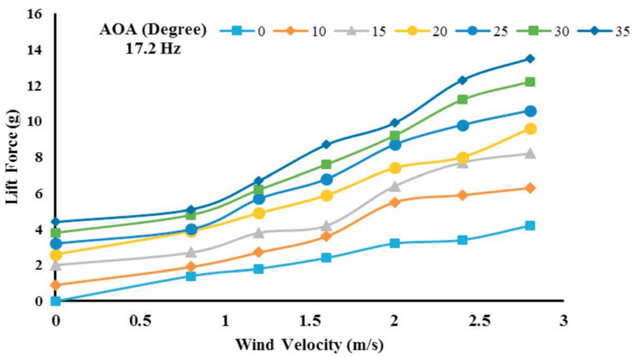

Figure 17. Lift force measurement in golden snitch ornithopter.

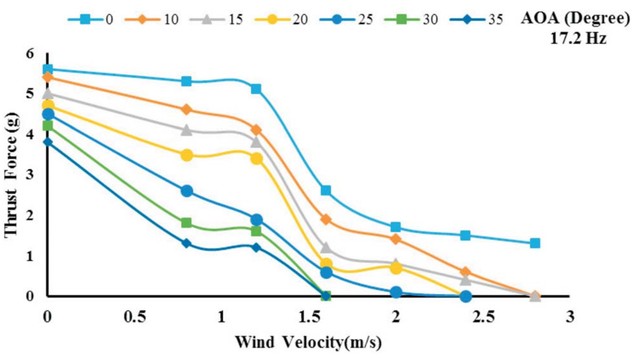

Figure 18. Thrust force measurement in golden snitch ornithopter.

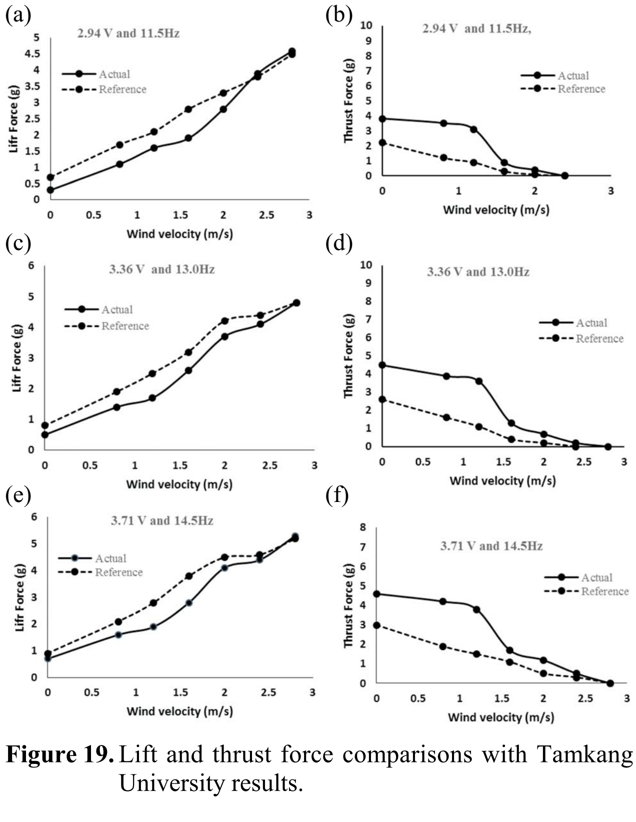

Figure 19. Lift and thrust force comparisons with Tamkang University results.

5. Conclusion

A low cost static test bench is developed to measure lift and thrust forces of FWMAVs. In order to minimize the turbulence effect, symmetrical aerofoil section is fabricated and calibrated load cells are attached mutually perpendicular to each other. Wind tunnel experiments are conducted at various wind velocities, flapping frequencies and AOA for E-Bird and golden snitch ornithopters. E-Bird has generated a maximum lift of 28.7 g at 60° AOA, 2.8 m/sec thrust of 12.3 g at zero AOA and zero wind velocity. Similar experiments with golden snitch Ornithopter of Tamkang University revealed that, at 35° AOA and 2.8 m/sec wind velocity, a maximum lift force of 13.5 g is obtained. Comparative evaluation of results at 39.6° stroke angle and 20° AOA suggested that, developed test rig measurement is in accord with Tamkang University results. The constructed bench test setup can be used to measure the lift and thrust forces of 0.1 g accuracy. Due to the utilization of low cost load cells, the cost of the rig is minimized in comparison with other test rigs.

Acknowledgements

The author would like to thank DRDO – AR & DB – SIGMA for providing financial support and SIGMA panel members for their valuable guidance.

References

[1] Willmott, A. P. and Ellington, C. P., "The Mechanics of Flight in the Hawkmoth Manduca Sexta. I. Kinematics of Hovering and Forward Flight," *Journal of Experimental Biology*, Vol. 200, No. 21, pp. 2705–2722 (1997).

[2] Gerdes, J. W., Gupta, S. K. and Wilkerson, S. A., "A Review of Bird-inspired Flapping Wing Miniature Air Vehicle Designs," *Journal of Mechanisms and Robotics*, Vol. 4, No. 2, p. 021003 (2012). doi: 10.1115/1.4005525

[3] Shyy, W., Aono, H., Chimakurthi, S. K., Trizila, P., Kang, C. K., Cesnik, C. E. and Liu, H., "Recent Progress in Flapping Wing Aerodynamics and Aeroelasticity," *Progress in Aerospace Sciences*, Vol. 46, No. 7, pp. 284–327 (2010). doi: 10.1016/j.paerosci.2010.01.001

[4] Tsai, B. J. and Fu, Y. C., "Design and Aerodynamic Analysis of a Flapping-wing Micro Aerial Vehicle," *Aerospace Science and Technology*, Vol. 13, No. 7, pp. 383–392 (2009). doi: 10.1016/j.ast.2009.07.007

[5] Fujikawa, T., Hirakawa, K., Sato, Y., Makata, Y. and Kikuchi, K., "Motion Analysis of Small Flapping Robot for Various Design and Control Parameters," IEEE International Conference on Robotics and Biomimetics, pp. 13–18 (2007). doi: 10.1109/ROBIO.2007.4522127

[6] Fenelon, M. A. and Furukawa, T., "Design of an Active Flapping Wing Mechanism and a Micro Aerial Vehicle Using a Rotary Actuator," *Journal of Mechanism and Machine Theory*, Vol. 45, No. 2, pp. 137–146 (2010). doi: 10.1016/j.mechmachtheory.2009.01.007

[7] Kim, D. K., Kim, H. I., Han, J. H. and Kwon, K. J., "Experimental Investigation on the Aerodynamic Characteristics of a Bio-mimetic Flapping Wing with Macro-fiber Composites," *Journal of Intelligent Material Systems and Structures*, Vol. 19, No. 3, pp. 423–431 (2007). doi: 10.1177/1045389X07083618

[8] Zakaria, M. J., Bayoumy, A. M., Elshabka and Abd Elhamid, O. E.. "Experimental Aerodynamic Characteristics of Flapping Membrane Wings," 13th International Conference on Aerospace Sciences & Aviation Technology, pp. 26–28 (2009).

[9] Wood, R. J., "Design, Fabrication, and Analysis of a 3 DOF, 3 cm Flapping-wing MAV," IEEE/RSJ International Conference on Intelligent Robots and Systems, pp. 1576–1581 (2007). doi: 10.1109/IROS.2007.4399495

[10] Harmon, R. L., "Aerodynamic Modeling of a Flapping Membrane Wing Using Motion Tracking Experiments," *ProQuest* (2008).

[11] Kuang, P. D., Dorothy, M. and Chung, S. J., "Robobat: Dynamics and Control of a Robotic Bat Flapping Flying Testbed," AIAA Infotech at Aerospace Conference, pp. 1435–1437 (2011). doi: 10.2514/6.2011-1435

[12] Curtis, D. H., Reeder, M. F., Svanberg, C. E., Cobb, R. G. and Parker, G. H., "Flapping Wing Micro Air Vehicle Bench Test Setup," *International Journal of Micro Air Vehicles*, Vol. 4, No. 1, pp. 51–77 (2012). doi: 10.1260/1756-8293.4.1.51

[13] Park, H. C., Priamadi, E. and Truong, Q. T., "Effect of Flapping-wing Kinematics on Force Generation," *International Journal of Intelligent Unmanned Systems*, Vol. 1, No. 3, pp. 245–255 (2013). doi: 10.1108/IJIUS-03-2013-0015

[14] Rose, C. and Ronald, S. F., "Comparison of Ornithopter Wind Tunnel Force Measurements with Free

Flight," IEEE International Conference on Robotics and Automation, pp. 1816–1821 (2014). doi: 10.1109/ICRA.2014.6907097

[15] Srigrarom, S. and Chan, W. L., "Ornithopter Type Flapping Wings for Autonomous Micro Air Vehicles," *Aerospace*, Vol. 2, No. 2, pp. 235–278 (2015). doi: 10.3390/aerospace2020235

[16] Abas, M. F. B., Rafie, A. S. B. M., Yusoff, H. B. and Ahmad, K. A. B., "Flapping Wing Micro-aerial-vehicle: Kinematics, Membranes, and Flapping Mechanisms of Ornithopter and Insect Flight," *Chinese Journal of Aeronautics*, Vol. 29, No. 5, pp. 1159–1177 (2016). doi: 10.1016/j.cja.2016.08.003

[17] Yang, L. J., "The Micro-air-vehicle Golden Snitch and Its Figure-of-8 Flapping," *Journal of Applied Science and Engineering*, Vol. 15, No. 3, pp. 197–212 (2012). doi: 10.6180/jase.2012.15.3.01

[18] Pope, A. and Goin, K. L., *High-speed Wind Tunnel Testing*, John Wiley & Sons, New York (1965).

[19] Yang, L. J., Ko, A. F. and Hsu, C. K., "Wing Stiffness on Light Flapping Micro Aerial Vehicles," *Journal of Aircraft*, Vol. 49, No. 2, pp. 423–431 (2012). doi: 10.2514/1.C031320

[20] Yang, L. J., Hsu, C. K., Han, H. C. and Miao, J. M., "Light Flapping Micro Aerial Vehicle Using Electrical-discharge Wire-cutting Technique," *Journal of Aircraft*, Vol. 46, No. 6, pp. 1866–1874 (2009). doi: 10.2514/1.38862

Manuscript Received: Oct. 17, 2017
Accepted: Feb. 27, 2018